Ecological Modelling 265 (2013) 207–220

Contents lists available at SciVerse ScienceDirect

Ecological Modelling

journal homepage: www.elsevier.com/locate/ecolmodel

Modeling the influence of flow on invertebrate drift across spatial scales using a 2D hydraulic model and a 1D population model

Kurt E. Anderson[a,*], Lee R. Harrison[b], Roger M. Nisbet[c], Allison Kolpas[d]

[a] Department of Biology, University of California, Riverside, CA 92521, USA
[b] NOAA Fisheries, Southwest Fisheries Science Center, 110 Shaffer Rd, Santa Cruz, CA 95060, USA
[c] Department of Ecology, Evolution, and Marine Biology, University of California, Santa Barbara, CA 93106, USA
[d] Department of Mathematics, West Chester University, West Chester, PA 19383, USA

ARTICLE INFO

Article history:
Received 10 April 2013
Received in revised form 6 June 2013
Accepted 9 June 2013
Available online 20 July 2013

Keywords:
Rivers
Dispersal
Drift
Macroinvertebrates
Spatial population dynamics
Environmental flow assessments

ABSTRACT

Methods for creating explicit links in environmental flow assessments between changes in physical habitat and the availability and delivery rate of macroinvertebrates that comprise fish diets are generally lacking. Here, we present a hybrid modelling approach to simulate the spatial dynamics of macroinvertebrates in a section of the Merced River in central California, re-engineered to improve the viability of Chinook salmon. Our efforts focused on quantifying the influence of the hydrodynamic environment on invertebrate drift dispersal, which is a key input to salmon bioenergetics models. We developed a two-dimensional hydrodynamic model that represented flow dynamics well at baseflow and 75% bankfull discharges. Hydraulic predictions from the 2D model were coupled with a particle tracking algorithm to compute drift dispersal, where the settling rates of simulated macroinvertebrates were parameterized from the literature. Using the cross-sectional averaged velocities from the 2D model, we then developed a simpler 1D representation of how dispersal distributions respond to flow variability. These distributions were included in 1D invertebrate population models that represent variability in drift densities over reach scales. Dispersal distributions in the 2D simulation and 1D representation responded strongly to spatial changes in flow. When included in the 1D population model, dispersal responses to flow 'scaled-up' to yield distributions of drifting macroinvertebrates that showed a strong inverse relationship with flow velocity. The strength of the inverse relationship was influenced by model parameters, including the rate at which dispersers settle to the benthos. Finally, we explore how the scale of riffle/pool variability relative to characteristic length scales calculated from the 1D population model can be used to understand drift responses for different settling rates and at different discharges. We show that, under the range of parameter values explored, changes in velocity associated with transitions between riffles and pools produce local changes in drift density of proportional magnitude. This simple result suggests a means for confronting model predictions against field data.

1. Introduction

Riverine systems are characterized by dynamic feedbacks among system components, a high degree of spatial and temporal variability, and connectivity among habitats. One of the most dominant influences on all of these features is the hydrodynamic environment, and a common conceptual theme is how changes to flow regimes alter the availability and spatial structure of physical habitat (Poff et al., 1997; Townsend, 1989; Vannote et al., 1980). Variability in flow can also shape biota by differentially affecting behavior, reproduction, and survival at different spatial scales. For example, the local distribution of invertebrates or fish may reflect behavioral responses to small scale variation in hydrodynamic parameters (Hart and Finelli, 1999; Lamouroux et al., 1999). In contrast, larger scale environmental variation (e.g. total habitat availability in a stream reach) may affect broader population- and community-level responses by altering rates of survival and reproduction (Daufresne and Renault, 2006; Hart and Finelli, 1999; Lytle and Poff, 2004; Woodward and Hildrew, 2002).

A major challenge is to identify ways of recognizing the myriad consequences of hydrodynamic variability in practical methodology for determining the flow requirements of instream populations and communities. Evaluations of how changes in flow will affect the viability of instream populations and communities, termed environmental flow assessments (EFAs), have traditionally relied on simple hydrological and habitat-association methods (Anderson et al., 2006b; Locke et al., 2008). Commonly used hydrological methods allocate discharge based on historic

* Corresponding author. Tel.: +1 951 334 8179.
E-mail address: kurt.anderson@ucr.edu (K.E. Anderson).

0304-3800/$ – see front matter © 2013 Elsevier B.V. All rights reserved.
http://dx.doi.org/10.1016/j.ecolmodel.2013.06.011

averages or physical habitat models that link habitat "suitabilities" for target species with hydraulic models that simulate availability of physical habitat as it varies across discharges (e.g. Milhous and Waddle, 2012). These methods explicitly consider only the tolerance of individuals in target populations to general flow and habitat variables (Anderson et al., 2006b), yet preserving the viability of managed populations and ecosystems is fundamental to modern EFA thinking (Arthington et al., 2006; Locke et al., 2008; Poff et al., 2010; Richter et al., 2006; Tharme, 2003). Further progress requires explicitly linking changes in the flow regime and habitat availability with population dynamics (Shenton et al., 2012), as population viability necessitates that additions of new individuals to the population exceed losses over the long term.

An important complication is that changes in flow affect target populations not only directly via abiotic factors, but also indirectly via biotic ones. Frequent targets of EFAs are fish, and bioenergetic models are often used to link flow with biotic processes in these contexts. A key biotic variable in fish bioenergetics models is food delivery rate (Chipps and Wahl, 2008; Ney, 1993; Pecquerie et al., 2011) which many studies assume to be either uniform or simple functions of velocity (e.g. see references in Hayes et al., 2007). Frequently missing are the known effects of physical habitat and flow on the dispersal and population dynamics of benthic macroinvertebrates (fish food) and feedbacks between fish and their prey. Recent notable attempts have been made to integrate flow variability, variability in food delivery rates and bioenergetics to model discharge-dependent fish biomass (e.g. Hayes et al., 2007). However, the combination of context dependence and computational expense hinders the ability of current approaches to scale-up results to whole reaches (i.e. 100s of meters) and beyond.

Recent theoretical advances have demonstrated that links between physical habitat, flow, and ecological responses can be understood in terms of characteristic length scales (reviewed in Anderson et al., 2006b). These length scales emerge as properties of a community of organisms interacting dynamically with their physical environment. Theory regarding characteristic length scales in rivers has generally addressed at least one of two themes: the minimal habitat required to sustain a viable population subject to downstream drift (Speirs and Gurney, 2001; Lutscher et al., 2005; Pachepsky et al., 2005), and the spatial scale over which the local environment is strongly affected by variability in upstream populations (Anderson et al., 2005, 2006a; Nisbet et al., 2007; Diehl et al., 2008). The second of these, termed the "response length", can describe the spatial scales over which population distributions are driven largely by dispersal and habitat selection shift to the scales where distributions are driven largely by survival and reproduction. Response lengths therefore potentially provide a means to predict how the distribution and abundance of target fish taxa and their prey change downstream of small scale habitat changes, such as a shift between riffle and pools, and larger scale changes such as downstream of dams.

Anderson et al. (2005) provided a recipe for calculating response lengths across a range of flow conditions using commonly collected data; this analysis was applied to multiple taxa in Diehl et al. (2008). Necessary data include invertebrate drift rates and consumption rates by fish as well as the distribution of dispersal distances observed during a drift event. However, almost all discussion in the papers cited above and in subsequent work was based on a one dimensional (1D) representation of flow, assuming parameters relate directly to some "mean" river velocity. The validity of this representation has yet to be tested against more accurate two or three dimensional flow representations, much less empirically. Determining the validity of 1D representations of flow-mediated dispersal is an important step in advancing the utility of characteristic length scale concepts in practical settings and preparing them for empirical testing.

Here, we simulate the spatial dynamics of benthic macroinvertebrates in a section of the Merced River in central California, re-engineered to improve the viability of juvenile and adult Chinook salmon. Macroinvertebrates are the sole salmon prey in the Merced River and thus are a key component of habitat quality. We focus our efforts on quantifying the influence of the hydrodynamic environment on invertebrate drift dispersal and densities using parameterized 2D and 1D models. Frameworks for simplifying computationally intense multidimensional models are used commonly in hydrological engineering (Wu, 2008), but come with additional challenges in ecology owing to complex behavior of drifting organisms (Fingerut et al., 2011; Oldmeadow et al., 2010), potentially explaining their absence from current EFA and bioenergetics modelling. To this end, we use experimental data from the literature to parameterize the settling rates of simulated "particles" in a 2D flow model, allowing us to construct simpler 1D representations of dispersal distributions. These distributions are used in 1D models and then 'scaled up' to represent variability in drift densities over reach scales. Finally, we explore how the scale of riffle/pool variability relative to the scale of the calculated response length can be used to understand drift responses for different settling rates and at different discharges.

2. Materials and methods

2.1. Study area

The focus of our modelling is the Robinson Reach, a recently re-engineered section of the Merced River in the central valley of California. Full details about the site can be found in C.A.D.W.R. (2005) as well as Albertson et al. (2011), Harrison et al. (2011), and Legleiter et al. (2011). In brief, the Robinson Reach was restructured and rescaled in 2001 as part of a larger effort to improve Chinook salmon habitat and channel-floodplain functionality following 150 years of gravel mining that had occurred at the site. The re-engineered channel has a single-thread, meandering planform, with alternating deep pools and shallow riffles. The average bankfull width is 29.2 m and the bankfull discharge is 42.5 m^3/s. The median grain-size is 52.5 mm, which is slightly smaller than nearby reaches not subjected to restructuring (Albertson et al., 2011). These and other channel features were specifically designed to avoid fine sediment build-up in riffles, thereby preserving the physical habitat suitability for Chinook salmon under a managed flow regime. The highly regular and well-ordered structure of the Robinson Reach provides us with a field-scale laboratory – similar to a flume – in which we can investigate the spatial dynamics of benthic macroinvertebrates under a variable flow environment with a minimum of confounding complexity.

2.2. Model descriptions

2.2.1. Overview of approach

We use a hybrid modeling approach that uses a 2D hydraulic model of flow dynamics, coupled with a simulation of invertebrate drift and settlement, to parameterize a 1D model of invertebrate population dynamics. First, we simulate the longitudinal and lateral flow field of the Merced River using a hydraulic model parameterized at baseflow and 75% bankfull discharges. These discharges were selected to represent typical low and high flow conditions on the river. The flow field is then coupled with a particle tracking algorithm that simulates the transport and settlement of individual macroinvertebrates that are the primary food source for young salmon across a riffle/pool sequence. Particle settling velocities are parameterized using published experimental data. We then use the streamwise distribution of distances traveled by particles to fit the dispersal representation of a 1D population model. Finally,

the model is used to simulate the spatial distribution of drifting invertebrates in the entire Robinson Reach at different parameter values and discharges. This combination of methods allows us to explore the influence of macroinvertebrate transport in a variable flow environment on dispersal distributions, drift densities, and related characteristic length scale calculations for the Merced River.

2.2.2. 2D hydrodynamic modelling

2.2.2.1. 2D hydrodynamic model. We used the hydrodynamic module in MIKE 21 Flow Model FM (D.H.I., 2011a) to characterize the 2D flow field in the longitudinal and lateral directions through the Robinson Reach. MIKE 21 solves the vertically-averaged and Reynolds-averaged equations representing the conservation of mass and momentum. The spatial discretization of the governing equations is performed using a cell-centered finite volume method. The MIKE 21 model assumes that the flow is hydrostatic (i.e. vertical velocity magnitudes and vertical velocity accelerations are small) and that turbulence is adequately represented by relating Reynolds stresses to shear via an isotropic eddy viscosity. The hydrostatic assumption is reasonable on the Robinson Reach where changes in bed slope are gradual along the direction of flow and field measurements indicate that the vertical velocity comprises a very small fraction of the total velocity magnitude (Harrison et al., 2011).

Turbulence is modeled using the concept of an eddy viscosity, which is calculated in both the vertical and horizontal directions (see Nelson et al., 2003, for a detailed description of the theory and reasoning behind using an eddy viscosity concept in two-dimensional flow modeling). The vertical eddy viscosity is assumed to be parabolic for the lower 20% of the flow depth and constant for the upper portion of the water column, resulting in a velocity profile that is logarithmic near the bottom and parabolic well away from the bed. The lateral eddy viscosity (LEV) parameter is used to represent horizontal momentum exchange due to turbulence not generated at the bed, but rather due to small-scale flow separation and eddies. Unlike the vertical eddy viscosity, the LEV is an adjustable parameter that can be specified within the 2D model. Using established LEV values that were developed in a prior 2D flow model application at this site (Harrison et al., 2011), we calculated the LEV as (Nelson and McDonald, 1996):

$$\mathrm{LEV} = 0.01\, v_{\mathrm{avg}}\, d_{\mathrm{avg}} \quad (1)$$

where v_{avg} and d_{avg} are the averaged velocity and depth, respectively, at the relevant discharges.

The model boundary conditions include input bed topography, specified upstream discharge and a downstream water surface elevation. In order to take advantage of existing hydraulic data sets, the MIKE21 FM model was calibrated and validated using a 2D flow model developed for the entire Robinson Reach, which included 10 bends of nearly uniform dimensions and curvature (see Harrison et al., 2011; Legleiter et al., 2011) for additional site description). Bed topography was surveyed across the active channel and roughly 10 m of the floodplain on either bank using a total station, with a mean cross section spacing of 7 m (20% of the channel width) and an average distance of 2 m between points along a transect. The topographic data was interpolated to form a continuous topographic surface using the specialized kriging method for curved channels by (Legleiter and Kyriakidis, 2008). The model runs utilized a mesh with a consistent grid node spacing of 1.0 m in the streamwise (x) and cross-stream (y) directions.

Water surface elevations (WSE) above the river bed were measured in the field at discharges of $Q = 6.4\ \mathrm{m^3/s}$ (baseflow conditions) and $Q = 32.5\ \mathrm{m^3/s}$ (~75% of the bankfull flow). Additional hydraulic data included 113 point measurements of velocity collected along six cross-sectional transects during a typical baseflow of $6.4\ \mathrm{m^3/s}$. Transects were placed among the first three riffles and bend pools in the upper portion on the reach; see Fig. 1 in Harrison et al. (2011) for exact locations. Velocity data were obtained with an acoustic Doppler velocimeter (ADV), which measured three-dimensional velocities for 60 s at a height above the bed equal to 40% of the local flow depth, approximating the depth-averaged velocity for an assumed logarithmic vertical profile, consistent with the hydrodynamic model.

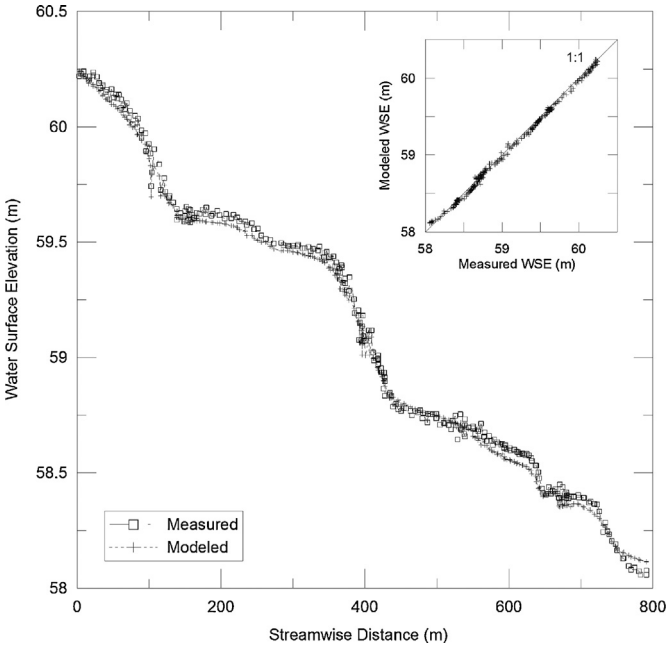

Fig. 1. Comparison between measured and modeled water surface elevations (WSE) for a discharge of $Q = 6.4\ \mathrm{m^3/s}$. The inset plot shows the observed versus predicted WSE and the minimal scatter about the 1:1 line. In this example, the drag coefficient $C_d = 0.017$ and the lateral eddy viscosity $LEV = 0.003\ \mathrm{m^2/s}$. The root mean square error RMSE between predicted and observed WSE is 0.038 m. For $Q = 32.5\ \mathrm{m^3/s}$, $C_d = 0.017$, $LEV = 0.01\ \mathrm{m^2/s}$, and WSE RMSE = 0.037 m.

The 2D hydrodynamic model was calibrated by adjusting the roughness, in the form of a drag coefficient (C_d), until the root mean square error (RMSE) was minimized between the measured and predicted water surface elevations. Overall agreement between modeled and measured water surface elevations was close, with RMSE values slightly less than 0.04 m (Fig. 1). To assess the accuracy of the flow model, we compared predicted vertically-averaged velocity magnitudes with the values measured at baseflow conditions; regression analyses produced a coefficient of determination $R^2 = 0.79$ and a RMSE between predicted and observed velocities that was roughly 20% of the mean flow velocity (Fig. 2). This good overall agreement suggests that the model is capable of reproducing the hydraulics at the Robinson Reach field site.

2.2.2.2. Particle tracking simulations. The goal of our particle tracking simulations was to characterize the influences of flow variability on the travel distances of individual macroinvertebrates across discharges. To do this, we utilized the MIKE 21 Flow Model FM Particle Tracking Module (D.H.I., 2011b). The particle tracking algorithm uses a Lagrangian discretization to predict the discrete pathways and travel distances of individual particles. The solution to the hydrodynamic model equations provides the framework for the particle transport calculations. Particles respond to the flow field solution as determined by input properties that include their settling velocity (ω_s) and horizontal and vertical dispersion rates (D_H and D_V, respectively).

Since the Robinson Reach possesses a repeating riffle/bend-pool channel morphology where the dimensions among morphologic units are highly consistent, particle tracking simulations were

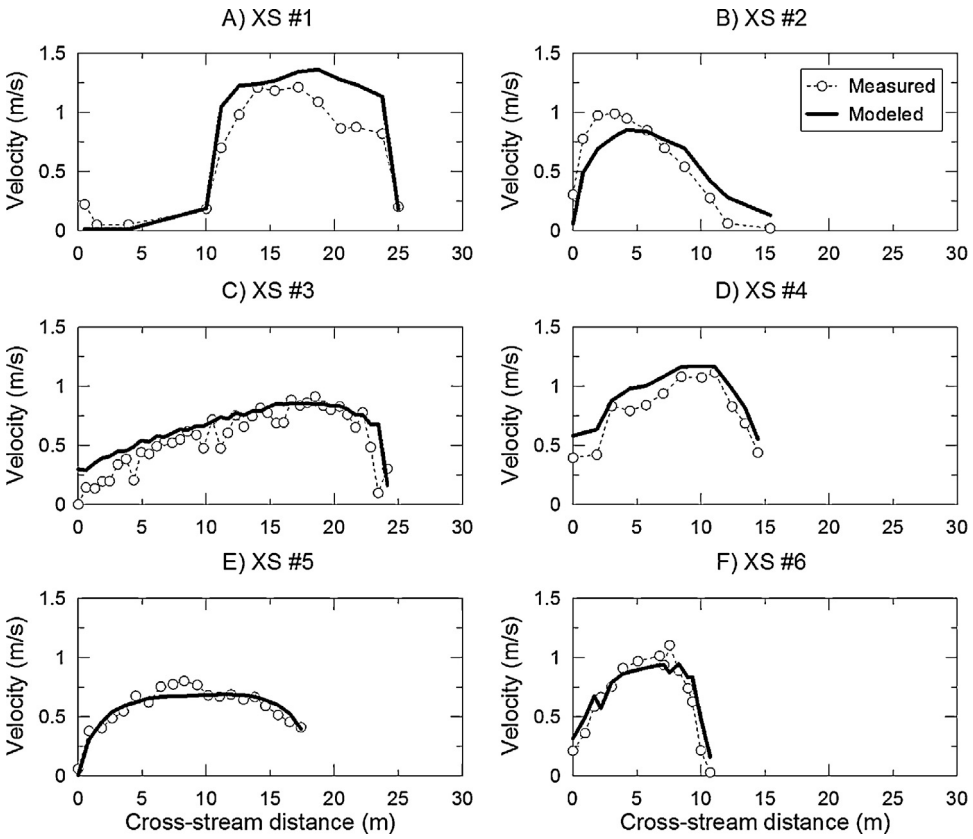

Fig. 2. Comparison between measured and modeled velocity magnitudes for a discharge of $Q = 6.4\,m^3/s$ across six cross-sectional transects in the Robinson Reach. The locations of the cross-sections (XS 1-6) are given in Harrison et al. (2011). The best fit linear regression $V_{obs} = 0.896 + 0.13\,V_{pred}$ ($n = 113$) yielded a coefficient of determination $R^2 = 0.79$.

completed over the lower seven bends to reduce computing time of the coupled flow-particle tracking simulations. At the beginning of each simulation, individual "macroinvertebrates" were introduced uniformly across the lateral axis of the upstream end of the flow model, which corresponded to the downstream edge of the third meander bend. In the absence of empirical data, we introduced invertebrates at 40% of the grid node depth to be consistent with the model predictions of the depth-integrated velocity, which is calculated at 40% of the flow depth. Furthermore, such a choice is at least consistent with reports of substantial drift densities in upper portions of the water column (also see Hayes et al., 2007). The concentration of organisms was computed at each node in the computational grid as the simulations progressed and the organisms were transported downstream. Drift transport was modeled using the flow models calibrated at discharges $Q = 6.4\,m^3/s$ (baseflow conditions) and $Q = 32.5\,m^3/s$ (~75% of the bankfull flow).

The effect of settling velocity (ω_s) and dispersion (D_H and D_V) have been shown to play important roles on the pattern of drift transport in previous models (Ciborowski, 1983; Hayes et al., 2007). An added complication arises from the fact that many stream macroinvertebrates exhibit control over their behavior in the drift and settle at rates that differ from similar sized inanimate particles (Allan and Feifarek, 1989; Campbell, 1985; Elliott, 1971a; Oldmeadow et al., 2010; Otto and Sjostrom, 1986). Because of this violation of the assumptions of Stoke's law, we estimated settlement velocities from published experiments on drift settlement (see Section 2.2.4.1). A particle was removed from the simulation once it encountered the benthic boundary.

In rivers, dispersion is generated by both horizontal eddies and vertically due to bed turbulence. Similar to the eddy viscosity concept, dispersion is defined as the product of a characteristic length scale and a velocity scale. Typically, the length and velocity scales are taken as the mean depth and velocity. Given the similarities in the functional form of their equations, dispersion coefficients (D_H and D_V) can be defined using a scaled eddy viscosity formulation with a typical scaling factor of one (D.H.I., 2011b; Rodi, 1993). Thus, we introduced particle dispersion as a random walk, where the input dispersion rates were set to the corresponding lateral eddy viscosities. Preliminary simulations showed that omitting the horizontal and vertical dispersion coefficients, either alone or in concert, could alter resulting drift patterns (data not shown). However, qualitative patterns most similarly matched those reported in empirical studies when dispersion coefficients matched the eddy viscosities (see Section 2.2.4.1), and were set as such for all remaining simulations and analyses.

2.2.3. 1D population model

2.2.3.1. Settlement model. Our approach to extending the results of the 2D particle tracking simulations to a population dynamic context is to use a set of 1D spatially-explicit partial differential equation models. We begin with an equation that simply describes the rate of change in the longitudinal density of drifting macroinvertebrates in terms of downstream transport and settlement to the stream benthos. Define $N_{Dvol}(x)$ as the number of drifting individuals per unit river volume at downstream distance x from a release point and at time t. Discharge Q is defined by the continuity equation as the product of the velocity v times the cross-sectional area A, where A equals the width w times the cross-sectional mean depth d. At constant discharge, $Q = v(x)A(x)$, where $v(x)$ is the spatially dependent downstream advection

velocity. Macroinvertebrates are transported downstream with velocity $v(x)$ and settle from the drift to the benthos at constant per capita rate σ (s^{-1}). Given a very small length of river h,

$$\underbrace{\frac{\partial}{\partial t}\left[hAN_{Dvol}(x)\right]}_{\substack{\text{rate of change}\\ \text{in drift density}}} = \underbrace{-\sigma hAN_{Dvol}(x)}_{\substack{\text{settlement}\\ \text{from drift}}} + \underbrace{QN_{Dvol}(x) - QN_{Dvol}(x+h)}_{\substack{\text{downstream}\\ \text{transport}}} \quad (2)$$

Let $N_D(x) = AN_{Dvol}$ be the density per unit river length. Making this substitution into Eq. (2), dividing through by h, and then taking the limit as h gets very small yields

$$\underbrace{\frac{\partial N_D}{\partial t}}_{\substack{\text{rate of change}\\ \text{in drift density}}} = -\underbrace{\sigma N_D}_{\substack{\text{settlement}\\ \text{from drift}}} - \underbrace{\frac{\partial}{\partial x}\left[vN_D\right]}_{\substack{\text{downstream}\\ \text{transport}}} \quad (3)$$

In the 1D model, the single parameter representing settlement rate, σ, and its inverse σ^{-1}, the mean time in the drift, aim to capture the combined effects of the settling velocity (ω_s), dispersion (D_H and D_V), and variations in flow and river channel morphology in the 2D model. The advection velocity, $v(x)$, represents the net longitudinal (streamwise) population displacement speed, and its value was chosen by using the continuity equation and solving for the cross-sectional average velocity $v(x)$ as Q/A along 1 m intervals for the entire 2D hydrodynamic model domain.

Given a constant point release at the upstream reach boundary $x = 0$ leading to a fixed density $N_D(0)$ of individuals at that point, Eq. (3) can be solved using elementary integrations to obtain the expected equilibrium density of drifting individuals at downstream location x,

$$N_D(x) = N_D(0)\frac{v(0)}{v(x)}e^{-\int_0^x \frac{\sigma}{v(y)}dy} \quad (4)$$

In a river with constant velocity $\bar{V}$ and depth $\bar{d}$, Eq. (4) simplifies to a negative exponential,

$$N_D(x) = N_D(0)e^{-\frac{\sigma}{\bar{V}}x}. \quad (5)$$

In this case, the average distance travelled is $\bar{x} = \bar{V}/\sigma$, which is equivalent to $\bar{V}\,\bar{d}/\omega_s$. Because we implement settlement in our model as a constant probability, individuals released from the same point will settle over a range of downstream distances (Anderson et al., 2012). The form of Eq. (5) has been used to model settlement in previous studies, providing reasonable fits to experimental releases of drifting macroinvertebrates (Elliott, 1971a; Lancaster et al., 1996; McLay, 1970).

Individual macroinvertebrates may of course emigrate into the drift and subsequently resettle many times in a lifetime. We thus implement a drift-benthos model that includes birth and death terms and that couples the drift settlement model (Eq. (2)) with an equation describing the dynamics of individuals residing on the benthos. Benthic density N_{Barea} is defined per unit benthic area (which equals the width w multiplied by length h), while drift density (N_{Dvol}) is defined per unit volume as above. These definitions lead us to the following balance equations:

$$\begin{aligned}
\underbrace{\frac{\partial}{\partial t}\left[hAN_{Dvol}(x)\right]}_{\substack{\text{rate of change}\\ \text{in drift density}}} &= \underbrace{\mu hwN_{Barea}(x)}_{\substack{\text{emigration}\\ \text{from benthos}}} - \underbrace{\sigma hAN_{Dvol}(x)}_{\substack{\text{settlement}\\ \text{from drift}}} - \underbrace{mhAN_{Dvol}(x)}_{\substack{\text{mortality}\\ \text{in drift}}}\\
&\quad + \underbrace{QN_{Dvol}(x) - QN_{Dvol}(x+h)}_{\substack{\text{downstream}\\ \text{transport}}}\\
\underbrace{\frac{\partial}{\partial t}\left[hwN_{Barea}(x)\right]}_{\substack{\text{rate of change in}\\ \text{benthic density}}} &= \underbrace{hR}_{\text{recruitment}} + \underbrace{\sigma hAN_{Dvol}(x)}_{\substack{\text{settlement}\\ \text{from drift}}} - \underbrace{\mu hwN_{Barea}(x)}_{\substack{\text{emigration}\\ \text{from benthos}}} - \underbrace{mhwN_{Barea}(x)}_{\substack{\text{mortality}\\ \text{on benthos}}}
\end{aligned} \quad (6)$$

We assume that new individuals recruit to the benthos at rate hR that is not dependent on benthic density, such as recruitment from egg banks laid by terrestrial adults. For simplicity, we assume that movement on the benthos is negligible and that per-capita mortality is similar on the benthos and in the drift. These assumptions can be relaxed in the framework we present here by, for example, allowing benthic individuals to exhibit diffusive or upstream biased movement (Elliott, 1971b, 2003; Englund and Hamback, 2004) or including separate per-capita mortality rates in the benthos and drift arising from differential predation (Dahl and Greenberg, 1996).

Rescaling Eq. (6) to obtain densities of benthic (N_B) and drifting (N_D) individuals per unit river length and following steps as outlined after Eq. (2) yields a 1D drift-benthos model similar to those employed in previous studies (Anderson et al., 2008; Kolpas and Nisbet, 2010; Lutscher et al., 2005; Pachepsky et al., 2005),

$$\begin{aligned}
\underbrace{\frac{\partial N_D}{\partial t}}_{\substack{\text{rate of change}\\ \text{in drift density}}} &= \underbrace{\mu N_B}_{\substack{\text{emigration}\\ \text{from benthos}}} - \underbrace{\sigma N_D}_{\substack{\text{settlement}\\ \text{from drift}}} - \underbrace{mN_D}_{\substack{\text{mortality}\\ \text{in drift}}} - \underbrace{\frac{\partial}{\partial x}\left[vN_D\right]}_{\substack{\text{downstream}\\ \text{transport}}}.\\
\underbrace{\frac{\partial N_B}{\partial t}}_{\substack{\text{rate of change in}\\ \text{benthic density}}} &= \underbrace{R}_{\text{recruitment}} + \underbrace{\sigma N_D}_{\substack{\text{settlement}\\ \text{from drift}}} - \underbrace{\mu N_B}_{\substack{\text{emigration}\\ \text{from benthos}}} - \underbrace{mN_B}_{\substack{\text{mortality}\\ \text{on benthos}}}
\end{aligned} \quad (7)$$

Equation (7) does not admit a closed form solution, but can be readily solved numerically. At equilibrium, this involves solving a simple first order ODE for drift density in x, where the initial upstream value can be set using drift rates of macroinvertebrates into the channel. Given a lack of such information for our system, we set the initial upstream value to the spatially homogenous equilibrium,

$$\bar{N}_D^* = \frac{R\mu}{m(m+\mu+\sigma)} \quad (8)$$

The equilibrium benthic density can then obtained from the simple relationship $\bar{N}_B^*(x) = \frac{R+\sigma\bar{N}_D^*(x)}{\mu+m}$. In the highly restrictive case where $R = 0$, Eq. (7) can be solved in a manner similar to Eq. (4) yielding

$$N_D(x) = N_D(0)\frac{v(0)}{v(x)}e^{-\int_0^x \frac{\phi}{v(y)}dy}, \quad \phi = \sigma + m - \frac{\sigma\mu}{\mu+m} \quad (9)$$

In a constant flow environment, $v(x)$ is replaced in Eq. (9) by $\bar{V}$. The quantity $\bar{V}/\phi$ then gives the spatial rate that a localized perturbation at $x = 0$ will decay downstream, which is referred to as the response length L_R of the system (Anderson et al., 2006a, 2005; Nisbet et al., 2007).

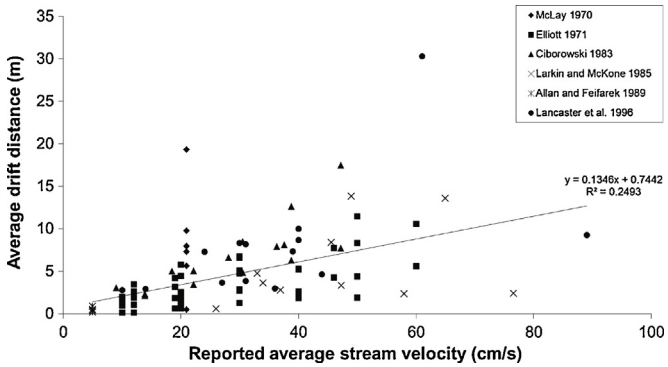

Fig. 3. Data used to estimate settlement velocities ω_s in the 2D hydraulic model. The linear equation represents the best-fit regression line for the aggregated data.

2.2.4. Data sources and parameter estimates

Values of parameters used in the 2D and 1D models are summarized in Table 1. Their sources and justification are described below.

2.2.4.1. Settlement velocities. We parameterized the settlement velocity ω_s in the 2D hydraulic model using a synthetic range of settling velocity values that were derived from the literature. We collected studies where drift distances were measured experimentally (Allan and Feifarek, 1989; Ciborowski, 1983; Elliott, 1971a; Lancaster et al., 1996; Larkin and McKone, 1985; McLay, 1970). Most of the organisms in these studies belonged to common stream macroinvertebrate taxa (i.e. mostly insects of the orders Ephemeroptera, Trichoptera, Plecoptera, Diptera, and Coleoptera, and crustaceans of order Amphipoda). Our selection of examples in no way represents a complete sample of relevant studies, and were conducted in many geographic regions, across a range of flow conditions, and under both field and laboratory experimental conditions. Rather, our goal was simply to generate a first cut at reasonable parameter values for model comparisons and to serve as a set of baseline calibrations for future empirical application.

All collected studies reported stream velocities, average drift distances (or its inverse, return rate), and stream depths. In some cases, release heights were reported; if not, we assumed that the release height was at a height above the bed equal to 40% of the local stream depth for consistency with our simulations. From these data, we were able to estimate settling rates σ (s^{-1}) as stream velocity/average distance traveled, and therefore settling velocity ω_s as settling rate × release height.

We estimated parameter values using 114 experimental drift releases in the cited studies. Macroinvertebrates in these studies collectively exhibited a strong positive relationship between their average distance traveled and stream velocity (Fig. 3), which is consistent with the assumptions of our particle tracking algorithm and 1D population models. Estimated settling velocities were $0.11 > \omega_s > 0.0011$ m/s, with most (86%) being less than or equal to 0.01 m/s. The average of these values was 0.0082 m/s while the median was 0.0042 m/s. Therefore, in order to span what we felt were reasonable and common values of settling velocities, we used $\omega_s = 0.0005$, 0.005, and 0.05 in our simulations. While some organisms did exhibit estimated settling velocities higher than 0.05 m/s, we found in preliminary runs that particles with these values mostly settled in their release node (i.e. within 1 m of the release point), even in the presence of horizontal and vertical dispersion.

In the absence of flow and geomorphic variability, the average settling rate can be approximated as $\sigma_{av} = \omega_s/(0.6\bar{d})$. The reach average depths were $\bar{d} = 0.52$ m and $\bar{d} = 0.90$ m for discharges $Q = 6.4\,m^3/s$ and $Q = 32.5\,m^3/s$, respectively. This yields settling rates of approximately $0.16\,s^{-1} > \sigma_{av} > 0.0016\,s^{-1}$ for $Q = 6.4\,m^3/s$ and $0.092\,s^{-1} > \sigma_{av} > 0.00092\,s^{-1}$ for $Q = 32.5\,m^3/s$.

2.2.4.2. Emigration, mortality, and recruitment. We estimated additional model parameters using a mixture of literature sources and unpublished data from the Merced River. Englund et al. (2001) used data from published experiments with benthic macroinvertebrates to estimate per capita emigration rates and per capita mortality rates due to consumption. The included experiments were open to immigration and emigration by the prey taxa. They demonstrated that, because of drift, only very small-scale (~1 m) experiments in the collection provided per capita emigration rates that can be interpreted in the same way as μ. Results from such experiments were limited to those from Dahl (1998a,b). Predators in these selected experiments were mostly fish (brown trout *Salmo trutta* and bullhead *Cottus gobio*), but also included one leech. Prey were invertebrates of the Family Chironomidae, Family Simuliidae, Order Ephemeroptera, and genus *Gammarus*.

Per capita emigration rates were presented in the presence and absence of predators, with marked differences between these. More relevant here are emigration rates reported in the presence of fish predators, as pikeminnow, sculpin, and salmon are common in the Robinson Reach. The range of these emigration rates in the selected experiments were $4.9 \times 10^{-5} > \mu > 2.5 \times 10^{-7}\,s^{-1}$; we assumed the median $\mu = 5.8 \times 10^{-6}\,s^{-1}$ represented a typical value. Consumption rates ranged from 0 to $4.8 \times 10^{-6}\,s^{-1}$. Assuming predation is the dominant source of mortality in our model and that the median of the non-zero consumption represents a typical value provides $m = 1.4 \times 10^{-7}\,s^{-1}$.

Recruitment rates for aquatic insects are somewhat more difficult to come by, but must balance mortality at equilibrium. The most prolific species in the Merced River are mayflies of the genus *Baetis*, with average benthic densities reported as $N_{Barea} = 1346\,m^{-2}$ and drift densities reported as $N_{Dvol} \approx 1.02\,m^{-3}$ (L. Albertson, unpublished data). As the average wetted width in the Robinson Reach at baseflow is $w = 19.8$ m and the cross-sectional area is $9.85\,m^2$, we obtain a longitudinal benthic density

Table 1
Summary of parameter values used in this study.

Parameter	Description	Value at baseflow	Value at 75% bankfull
Q	Discharge	$6.4\,m^3/s$	$32.5\,m^3/s$
ω_s	Settling velocity	0.0005, 0.005, 0.05 m/s	0.0005, 0.005, 0.05 m/s
D_H, D_V	Horizontal and vertical dispersion	$0.003\,m^2/s$	$0.01\,m^2/s$
$\bar{d}$	Reach average depth	0.52 m	0.90 m
$\bar{V}$	Reach average velocity	0.65 m/s	1.32 m/s
σ_{av}	Settling rate calculated from average conditions	0.0016, 0.016, $0.16\,s^{-1}$	0.0092, 0.092, $0.92\,s^{-1}$
σ_{est}	Settling rate estimated from 2D model results	0.0098, 0.011, $0.058\,s^{-1}$	0.0082, 0.0097, $0.029\,s^{-1}$
μ	Per capita emigration rate	$5.8 \times 10^{-6}\,s^{-1}$	$5.8 \times 10^{-6}\,s^{-1}$
M	Per capita mortality rate	$1.4 \times 10^{-7}\,s^{-1}$	$1.4 \times 10^{-7}\,s^{-1}$
R	Recruitment rate	0.0035 ind./m/s	0.0035 ind/m/s
$\bar{N}_D^*$	Equilibrium reach average drift density	14.8, 13.0, 2.49 ind./m	17.7, 14.9, 5.0 ind./m
L_R	Response length	2818, 2464, 473 m	6817, 5742, 1931 m

of $N_B \approx 26{,}651\,\mathrm{m}^{-1}$ and drift density of $N_D \approx 10\,\mathrm{m}^{-1}$. Setting recruitment $R = 0.0035$ ind./m/s provides spatially-homogenous equilibrium benthic and drift densities from Eq. (8) in the neighborhood of the empirically observed values.

2.3. Model analyses

2.3.1. Comparing travel distances between 1D and 2D models

The travel distances of individual particles were calculated and pooled to assess the downstream removal rate of drifting individuals for comparison with Eqs. (4) and (5). Drift and settlement locations were converted to streamwise values in ArcGIS to facilitate linkages with 1D models.

The settling behavior of particles in our 2D simulations was determined by the host of factors included in the particle tracking model, the complexity of which hindered straightforward transference of parameter values between 2D and 1D models. We therefore estimated the appropriate settling rate σ_{est} for a comparable 1D model using least-squares fitting; i.e. by minimizing the sum-of-squared residuals between Eq. (4) and the results from the particle tracking model. Given the estimated settlement rate, the average distance traveled $\bar{x}$ was determined numerically as the raw moment of Eq. (4),

$$\bar{x} = \frac{\int_0^\infty x N_D(x)\,dx}{\int_0^\infty N_D(x)\,dx}, \tag{10}$$

where the denominator provides the necessary normalization. Numerical tests demonstrated that the integrals in Eq. (10) always converged with the upper limit to integration set to less than the maximum downstream location in the Robinson Reach, $x = 1756$ m, making this value our practical integration limit. Estimates from Eq. (10) were compared with those from Eq. (5) parameterized using σ_{av}.

2.3.2. Population responses to flow variability in the 1D model

Relating flow dynamics and drift availability is a desired goal of bio-energetic and EFA modeling. To this end, we used the drift-benthos Eq. (7) – parameterized with values of the settling rate σ_{est} and estimates derived from the literature – to simulate equilibrium population responses to flow velocity variation along the modelled reach. Mechanisms responsible for the resulting spatial distributions were further clarified by means of spectral analysis and Fourier transforms. Here, Fourier transforms allow us to approximate both variation in the flow environment and the distribution of population density as a sum of sinusoids with different spatial wavelengths L_E. This effectively breaks arbitrarily distributed variability into larger-scale and smaller-scale components. For linear systems, the Fourier transformed variables can be related algebraically via a transfer function, thus providing a simple analytic expression between the input environmental variability and the output population distribution. Applications of these techniques in stream ecology contexts can be found in (Anderson et al., 2006a, 2005; Nisbet et al., 2007).

The specific form of the downstream transport term makes Eq. (7) non-linear. In order to proceed, we approximated Eq. (7) near equilibrium by re-writing it in terms of small deviations from spatial average equilibrium values $v(x) = \bar{V} + v_d(x)$, $N_B(x) = \bar{N}_B^* + n_B(x)$, $N_D(x) = \bar{N}_D^* + n_D(x)$. After making these substitutions and ignoring non-linear terms, we obtained the linearized system

$$\begin{aligned} \frac{\partial n_D}{\partial t} &= \mu n_B - \sigma n_D - m n_D - \bar{V}\frac{\partial n_D}{\partial x} - \bar{N}_D^*\frac{\partial v_d}{\partial x} \\ \frac{\partial n_B}{\partial t} &= \sigma n_D - \mu n_B - m n_B \end{aligned}. \tag{11}$$

The spatial Fourier transforms of velocity, benthic and drift density deviations are given by

$$\tilde{v}_d(L_E) = \int_{-\infty}^{\infty} v_d(x) e^{-\frac{2\pi i x}{L_E}}\,dx, \quad \tilde{n}_B(L_E) = \int_{-\infty}^{\infty} n_B(x) e^{-\frac{2\pi i x}{L_E}}\,dx,$$

$$\tilde{n}_D(L_E) = \int_{-\infty}^{\infty} n_D(x) e^{-\frac{2\pi i x}{L_E}}\,dx. \tag{12}$$

Applying the transforms in Eqs. (12) to (11) and re-arranging terms provides the transfer function relating variation in flow velocity and drift density,

$$T_V(L_E) = \frac{\tilde{n}_D}{\tilde{v}_d} = -\frac{1}{\phi}\frac{\bar{N}_D^*\frac{2\pi i}{L_E}}{1 + 2\pi i\frac{L_R}{L_E}} \tag{13}$$

where ϕ and L_R are as defined in Eq. (9) and i is $\sqrt{-1}$.

The transfer function $T_V(L_E)$ is a complex-valued function whose modulus is the ratio of amplitudes between the velocity variability v_d and the drift density variability n_D at the given spatial wavelength L_E. It is therefore a measure of the degree to which each scale of spatial variability in flow velocity is reflected in the distribution of drift densities.

3. Results

3.1. 2D flow-drift modelling

Fig. 4 shows maps of the spatial patterns in flow depth and velocity for the model reach at each simulated discharge condition. At $Q = 6.4\,\mathrm{m}^3/\mathrm{s}$, the flow was shallow in riffles and gradually deepened as the morphology transitioned from the riffle into the pool (Fig. 4a and b). The velocity field was also more uniform throughout the riffles and a high velocity core developed as flow was converged by a point bar located on the inner bank of the meander bend. Flow decelerated as it moved through the pool due to the expansion in width at the pool exit, which created a divergent flow field. At $Q = 32.5\,\mathrm{m}^3/\mathrm{s}$, a more well-developed high velocity core was present through the central portion of the riffles and through the pool thalweg, with velocities exceeding 1.5 m/s (Fig. 4c and d). Patterns observed at both discharges were repeated across riffle-pool sequences in the Robinson Reach.

At low flow, the predicted particle pathways followed the modeled velocity streamlines. Particles tended to exhibit parallel paths in riffles that then converged in pools. Instantaneous particle velocities also reflected the local velocity conditions as the particles traveling near the channel margins tended to settle out of the drift while particles located in the central portion of the channel are swept into the high velocity core and transported through the pool. During high-flow, the particle transport pathway followed a similar trajectory along the high velocity core. Drift concentrations were greatest in the channel centerline, though the zone of invertebrate transport occupies a greater fraction of the channel width.

Despite sharing the same properties, particles with the same settling velocities in the same discharge environment still settle out over a range of distances (Fig. 5). This reflected variation in lateral starting locations, depth and velocity variation, and particle dispersion. Preliminary simulations of particles without dispersion exhibited much less variation in downstream travel distances, although some variation remained due to interactions among flow variability, channel morphology, and different initial particle locations (not shown). Interestingly, results from simulations with high settling velocity ($\omega_s = 0.05$ m/s) differ markedly from those with lower settling velocities ($\omega_s = 0.005$ and 0.0005 m/s) at both

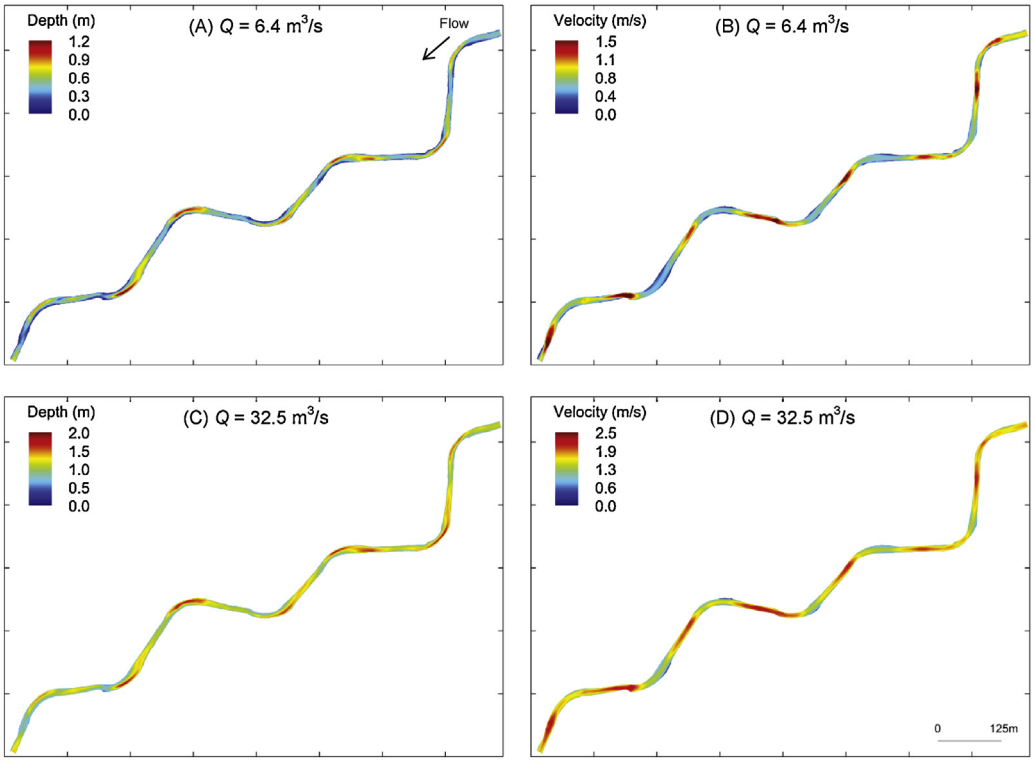

Fig. 4. Modeled depth and velocity for discharges of $Q = 6.4\ m^3/s$ (a and b) and $Q = 32.5\ m^3/s$ (c and d). Particles were introduced into the upper end of the reach (top right corner of each plot) and transported downstream with the flow, which travels from right to left. Pools are located in the curved portions of the channel and are separated by straight riffles.

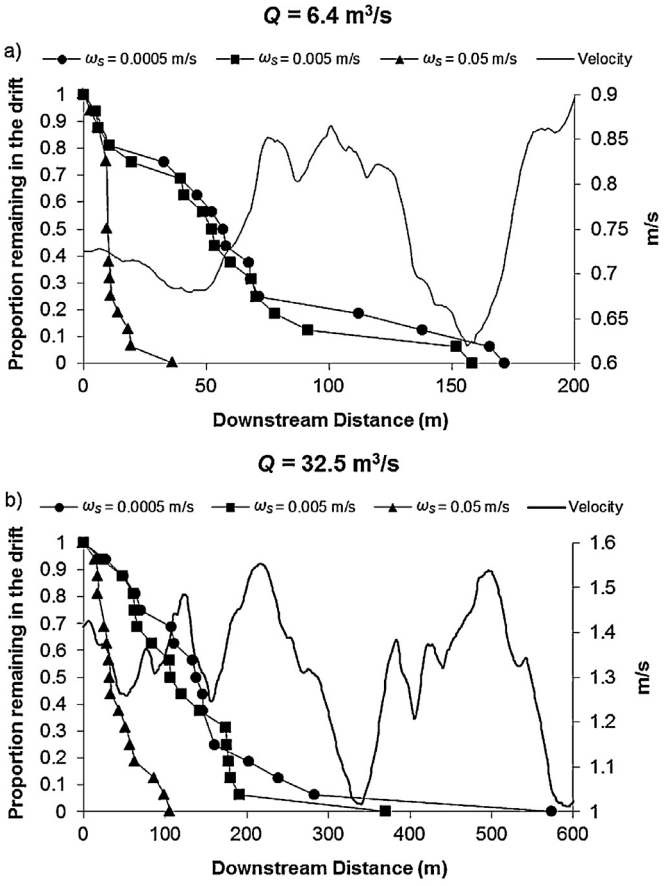

Fig. 5. Downstream drift of particles in the 2D hydraulic model superimposed over cross-sectional average velocities. (a) $Q = 6.4\ m^3/s$. (b) $Q = 32.5\ m^3/s$.

discharges. At lower settlement velocities, sinking appeared to be relatively weak compared to vertical and horizontal dispersion, with the latter moving particles in and out of the high velocity core due to turbulent fluctuations about the streamline pathway. In these cases, settlement was dictated to a great extent by both topography and flow turbulence. In contrast, the distances traveled by the farthest drifting particles differ dramatically among all simulations. For these particles, the influence of drift in the high velocity core appears to be particularly strong.

3.2. Linking particle tracking results with the 1D model

3.2.1. Cross-sectional average velocities

The overall longitudinal structures of the cross-sectional average velocities mirror those of the full 2D model (Fig. 6). The periodic

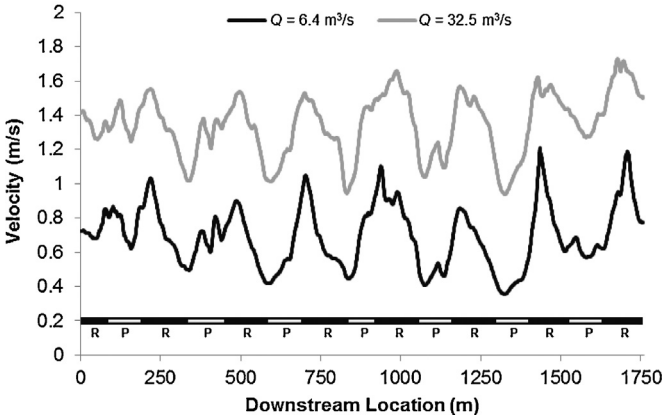

Fig. 6. Cross-sectional average velocities. The approximate locations of riffles are denoted by *R*, while *P* denotes bend pools.

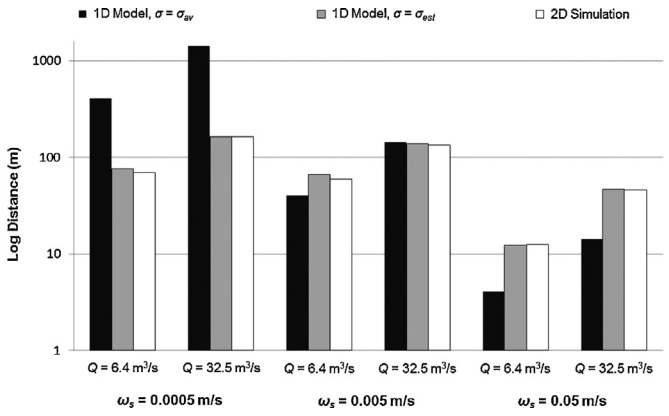

Fig. 7. Average distances traveled in the drift. Results from the particle tracking simulation in the 2D hydraulic model are compared to results of the 1D models. The "1D Model, $\sigma = \sigma_{av}$" is Eq. (5) parameterized by input settlement velocities ω_s, average river depths $\bar{d}$, and average river velocities $\bar{V}$. The "1D Model, $\sigma = \sigma_{est}$" is Eq. (4) fit to the 2D settlement results.

patterns in velocity that occur at the two discharge levels reflect the riffle/pool structure of the Robinson Reach. In general, high velocity stretches correspond to riffle habitats (Fig. 4b and d). The slight increase in velocity over the last 200–300 m downstream reflects a constriction in cross-sectional area due to gravel bar development. Harmonic means of the 1D velocity profiles are ~0.65 and ~1.32 m/s for baseflow and 75% bankfull conditions, respectively.

3.2.2. Settlement rates and average dispersal distances

Settlement rates σ_{est} estimated from fits to the 2D particle traces vary less than an order of magnitude within each discharge level (Table 1). For $Q = 6.4\,m^3/s$, settlement velocities $\omega_s = (0.0005, 0.005, 0.05)\,m/s$ correspond to settlement rates $\sigma_{est} = (0.0098, 0.011, 0.058)\,s^{-1}$, respectively. For $Q = 32.5\,m^3/s$, settlement velocities $\omega_s = (0.0005, 0.005, 0.05)\,m/s$ correspond to settlement rates $\sigma_{est} = (0.0082, 0.0097, 0.029)\,s^{-1}$.

Solutions of the separate parameterizations of the 1D model differ substantially in their match to the output from the 2D particle tracking simulations. The average downstream distances traveled by particles in the 2D simulations vary in a way that is entirely consistent with changes in settlement velocity and discharge (Fig. 7). Patterns produced from each parameterization of the 1D model also predictably follow changes in settlement velocity and discharge. However, the 1D model with dependence of drift on stream velocity (Eq. (4)) and a settling rate parameter estimated from the 2D results (σ_{est}) reproduces very well the average particle tracking travel distances across all settlement velocities and discharges. In contrast, the 1D model parameterized with σ_{av} in Eq. (5) can only reproduce qualitative patterns. This model – using reach average depths and no variability in velocity – dramatically overestimates the 2D average particle distances at low settling velocities and under estimates them at high ones. The details of particle behavior clearly influence the average settling rates, making them deviate from predictions based on average channel morphology and velocity. Yet once the settling rate σ is empirically recalibrated to account for these effects, predictions from the 1D model are quite accurate.

3.3. 1D model results

By modelling the effects of flow on macroinvertebrate drift and settlement, we seek to understand how changes in flow conditions alter the availability of macroinvertebrates in the drift. The 1D model, validated against the 2D simulation, allows us to make a series of predictions relating flow variability and drift availability.

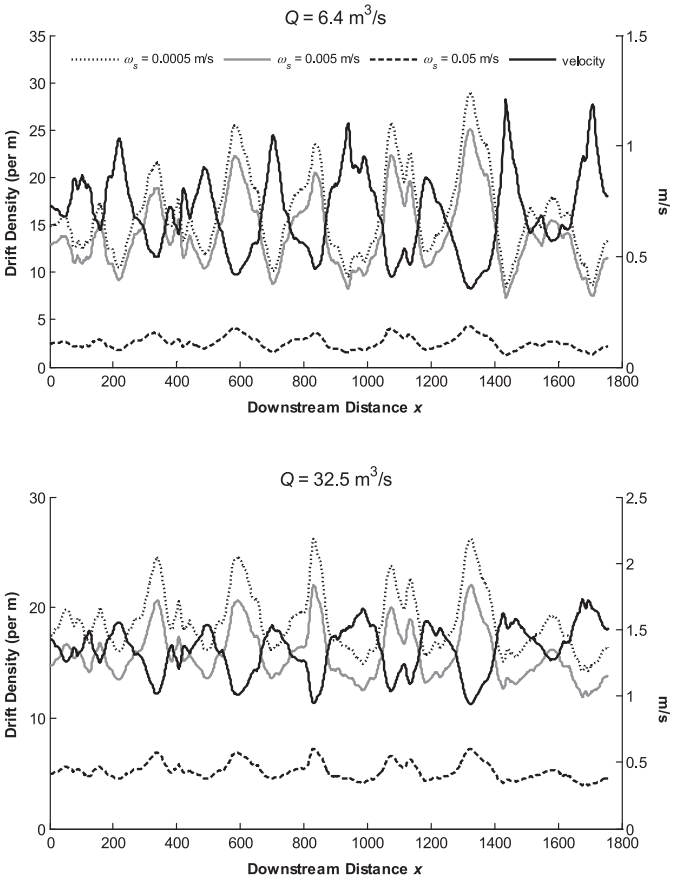

Fig. 8. Cross sectional average velocities and resulting equilibrium drift densities simulated using Eq. (7). Upstream values at $x = 0$ were set to the spatially uniform equilibrium values Eq. (8). Parameter values are as described in Table 1.

These predictions include both changes in the spatial average drift availability as well as how deviations from average velocity conditions alter drift densities locally. We focus on drift densities because they are common inputs to fish bioenergetic models, but recall that the equilibrium benthic density is simply a linear transformation of drift density.

3.3.1. 1D model simulations

Fig. 8 presents equilibrium drift densities over the entire Robinson Reach obtained from numerical simulations of Eq. (7) parameterized with σ_{est}. Reach-average densities of individuals in the drift decrease when settling velocities ω_s, and hence settling rates σ_{est}, are higher. Examination of Eq. (8) confirms that increases in σ_{est} in turn lead to lower reach-average drift densities at both discharges levels, as increasing σ_{est} leads to invertebrates spending less time in the drift. Differences between the two discharge levels result from the indirect effects of flow on σ_{est}. Thus, all else being equal, the rank order of σ_{est} gives the rank order of reach-average drift densities, regardless of discharge. Simulations also show that variation in drift density negatively tracks variation in flow velocity under all parameter combinations. Individuals moving through higher velocity areas will simply do so faster, leading to lower local densities. However, the strength of the relationship between velocity and drift density changes with changing ω_s and hence σ_{est}. As σ_{est} increases and individuals spend less time in the drift, local increases in flow velocity lead to less dramatic decreases in drift density at both discharge levels.

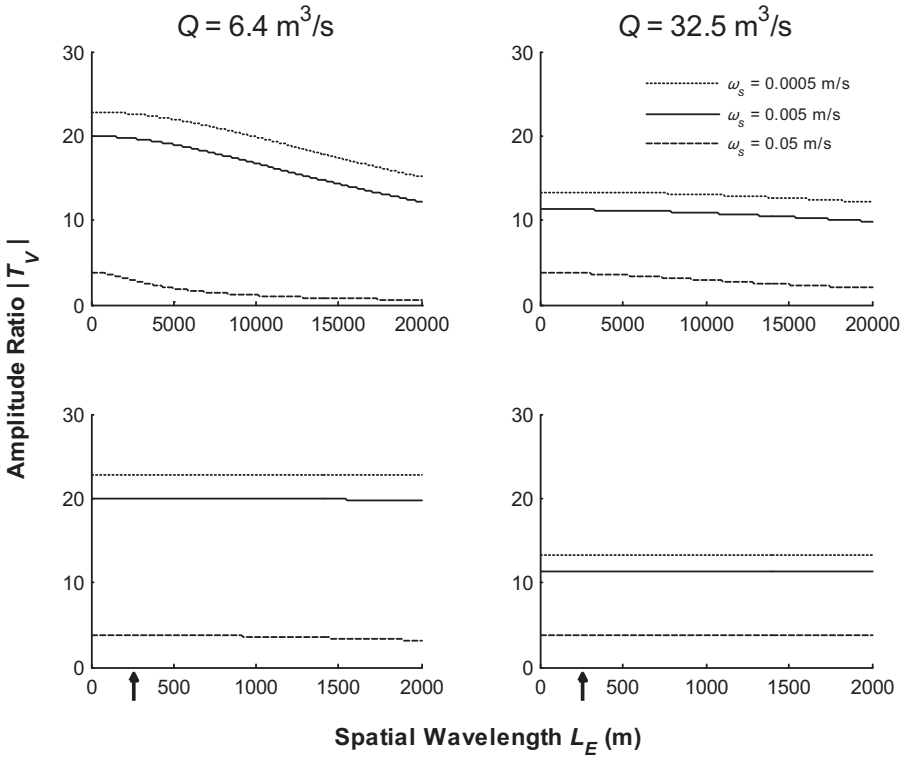

Fig. 9. The modulus of the transfer function, $|T_V|$, from Eq. (13) yields the ratio of amplitudes between variability in the flow velocity and variability in drift density at each spatial wavelength L_E. The upper panels present the amplitude ratio over a large wavelength range to highlight differences of this response among parameter values. The amplitude ratio is presented over a much shorter wavelength range that is most relevant to the scale of the Robinson Reach in the lower panels. Arrows on the lower panels point to the dominant scale of flow variability generated by riffle/pool transitions.

3.3.2. Drift responses to flow variability as revealed by transfer functions

The relationship between flow variability and drift density evident in the numerical studies can be further understood by examination of the output from the transfer function (Eq. (13)). This equation possesses a form similar to others relating variation in movement rates to population distributions examined by Anderson et al. (2005, 2006a) and Nisbet et al. (2007). In particular, drift densities show the strongest spatial response to small wavelength variation in flow velocity, approaching $\bar{N}_D^*/\bar{V}$ as $L_E \to 0$, and increasingly average larger wavelength variation, going to zero as $L_E \to \infty$. Because ω_s directly influences the value of $\bar{N}_D^*$ via σ_{est}, simple calculations confirm a direct, quantitative correspondence between the ratios of the reach-average drift density to the velocity from the numerical results in Fig. 8 and the outcomes predicted by the transfer function.

The spatial scale of transition between the minimum and the maximum population responses described above is controlled by the ratio of the response length to the wavelength of variation, L_R/L_E. The long, mostly km magnitude response lengths calculated across discharge and settlement values lead to transitions between minimum and maximum values in the transfer function that occur over 10s of km. The power spectrum of velocity variation reveals that by far the greatest wavelength component arises from differences between riffles and pools. Riffle-pool sequences are highly regular in the Robinson Reach, emerging at a spatial wavelength $L_E = 251$ m. The result when substituting this quantity into Eq. (13) shows that drift responses are very close to their maximum values regardless of settling velocity or discharge (Fig. 9). Thus, large changes in response lengths actually have a very small influence on the drift response over the range of parameters we examine here. Thus, we arrive at the simplifying result that, for organisms that disperse often, local changes in velocity produce local changes in drift density of proportional magnitude.

We can recast the result above in a way that facilitates confrontation with field data. Recognizing the result above, we define a sensitivity index yielding the fractional change in local equilibrium drift density resulting from a local fractional change in velocity,

$$\alpha_{NV} = \frac{V(x)}{N^*(x)} \frac{\partial N^*(x)}{\partial V(x)} = \frac{\partial \log N^*(x)}{\partial \log V(x)} \tag{14}$$

where $\alpha_{NV} \approx -1$ when $\mu \gg m$. Sensitivities defined as above can serve as regression coefficients (Fig. 10). Thus, Eq. (14) presents a baseline expectation; deviation from this predicted slope could reveal that other processes, for example velocity-driven changes in per capita emigration and mortality rates, are critical in determining drift availability.

4. Discussion

Flow models are typical components of environmental flow assessments. Forecasting effects of flow on invertebrate drift is an increasingly important objective of EFAs, complementing the well-established approaches that focus on documenting the influences of flow on the availability of physical habitat suitable for some species of interest. Here, we employed a hybrid of 2D and 1D modelling methods in an effort to determine the ability of simple models to capture the effects of the flow environment on drift dispersal. We found that certain one-dimensional representations of flow variability retained key structural components of our full 2D hydraulic model. These 1D models require substantially less processing time relative to full 2D representations, which in turn allows flow data to be linked to models of invertebrate population dynamics with a minimum of computational complexity.

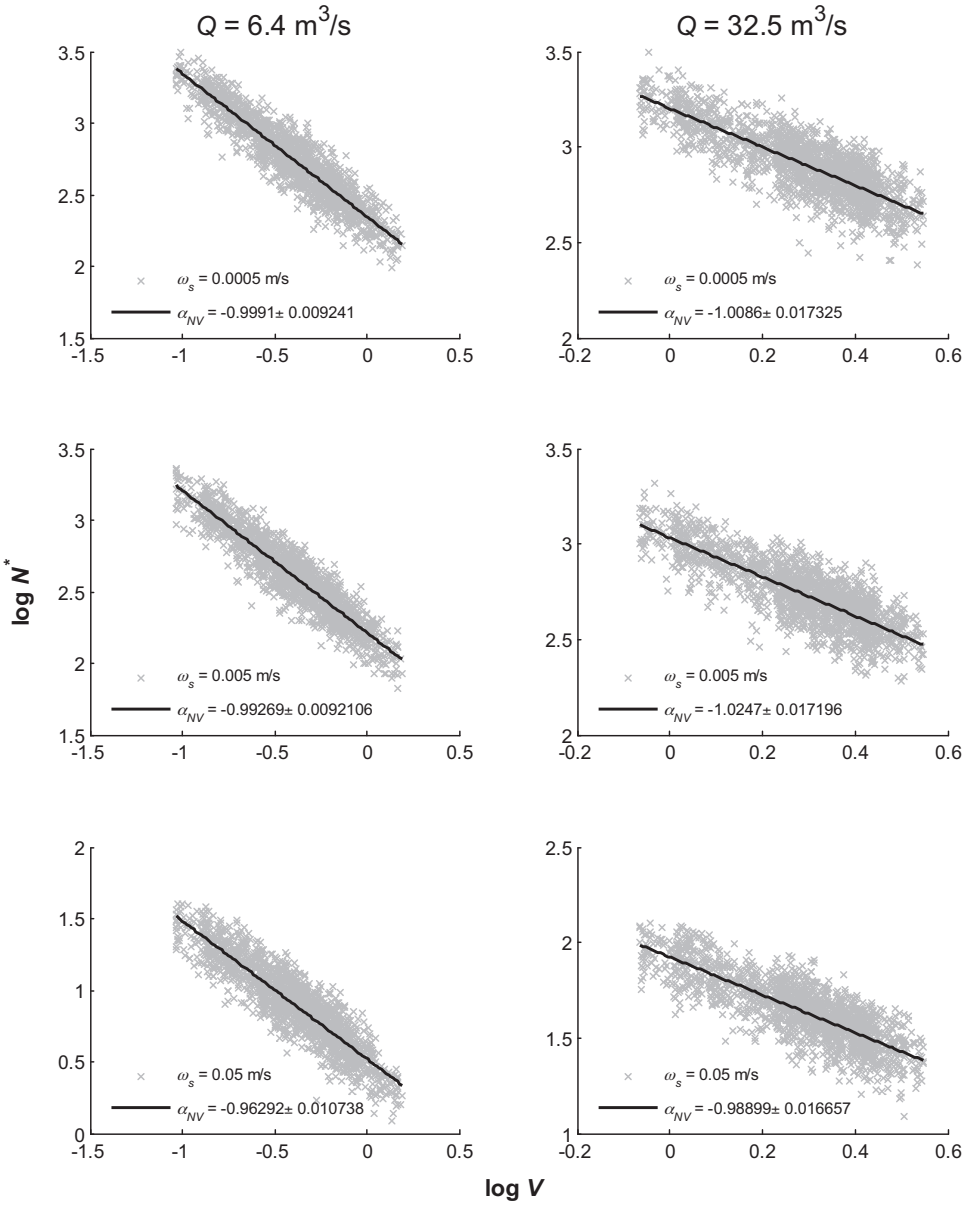

Fig. 10. Log-transformed drift densities and velocities show a consistent relationship across flow conditions. Drift densities are generated from values used in Fig. 8 with 10% C.V. added to simulate sampling error. The sensitivity parameter α_{NV} is obtained as the slope of a best-fit line $\log N^* \sim \alpha_{NV} \log V + \beta$, and is presented ±1 S.E. Coefficients in the linear model were estimated using least squares minimization.

Our hybrid approach therefore provides a way to 'scale-up' highly-resolved or well-parameterized descriptions of drift availability to temporal and spatial scales where fine resolution is not feasible.

In the context of EFAs, the model output that we have presented serves as a way to calibrate spatial variability in food availability, the "input" variable to fish bioenergetics models. Bioenergetic models are typically used to assess performance of individual fish across gradients of physical habitat variables and food availability (e.g. Rosenfeld and Taylor, 2009). With additional assumptions, they have been used to predict larger spatial patterns of biomass distribution or capacity (Grossman et al., 2002; Hayes et al., 2007; Hughes, 1998), but a remaining challenge is linking spatial patterns of growth and survival to population viability (Anderson et al., 2006b; Armstrong and Nislow, 2012; Frank et al., 2011; Locke et al., 2008). Individual-based modeling (IBM) approaches based on the bioenergetics of specific life stages for individual fish have been the most successful at this integration and have shown great utility in river management contexts (Van Winkle et al., 1998; Vincenzi et al., 2008). Most current IBMs are parameter rich, requiring extensive data and/or natural history knowledge of the particular system for calibration (Breckling et al., 2006). However, our 1D representations open the way to applying IBMs at much larger spatial scales, a consequence of which is that it becomes essential to have bioenergetic models that describe the full life cycle of a migratory fish such as salmon. One approach uses dynamic energy budget (DEB) theory (Kooijman 2010), which starts from a "standard", parameter-sparse, model structure; adding a small number of additional species-specific parameters captures significant intra- and interspecific variation in life history traits (Nisbet et al., 2012; Pecquerie et al., 2011). Linking a DEB model with habitat variation at large spatial scales still requires integrating up local, small scale information on foraging (Hayes et al., 2007) or territorial size (Ayllon et al., 2012) to allow specification of reach-level dynamics, but with potentially less computational cost than other methods.

We view the Robinson Reach as a field scale laboratory for investigating the relation between the flow and invertebrate transport

patterns in a simple river system. In this sense our approach is similar to using a lab flume but conducted at a larger spatial extent. The Robinson Reach is in the early stages of developing morphology that is more variable than the initial design state, yet the flow field does not possess the complexity observed in other rivers where physical structures, such as boulders or large wood, are present (Harrison et al., 2011). Because creation of structural complexity is a common restoration strategy for streams and rivers (Bernhardt et al., 2005), an extension of our work might consider the introduction of some small level of additional physical habitat complexity. Addition of large woody debris is particularly popular, as low velocity wakes create pool habitats (Abbe and Montgomery, 1996; Gurnell et al., 2002) that could increase retention of drifting invertebrates in the same manner as has been shown for sediments and nutrients. Modeling changes in flow and invertebrate transport around woody debris and other structural features could provide vital insight into the value of particular addition strategies and the scale over which they must be undertaken to provide marked positive influence on fish habitat.

For particularly complex hydrological environments, it is likely to prove impractical to simplify the entire domain into a 1D problem. However, we are still left with the issue of managing computational complexity. A potential solution would be an extension of our hybrid approach where linked models of differing spatial dimensionality handle different levels of flow complexity (Wu, 2008). A large river system would be broken up into subsections; areas of highly complex flow (e.g. near large woody debris or boulders, through braided channels) would be modeled using 2D or 3D models. Single dimension models would then be used for surrounding reaches that have less complexity, such as nearly straight channels or simple riffle/pool sequences. The only additional mathematical challenge beyond what we have presented here is proper specification of boundary conditions between model sections. Areas where models are integrated may emerge as foci for field calibration efforts to enhance linkages and reduce error propagation.

We have omitted some aspects of biological complexity that could potentially expand the ability of our 1D model to predict the availability of macroinvertebrate food to young salmon. First, future studies might incorporate additional behavior in the "particles" that represent drifting animals, for instance by coupling individual-based simulations with hydraulic models. While many stream organisms may drift and settle passively (Elliott, 1971a), many others actively swim or reposition their bodies in the drift (Allan and Feifarek, 1989; Campbell, 1985; Oldmeadow et al., 2010; Otto and Sjostrom, 1986). Settlement patterns may also be complicated by small-scale hydrology (Fonseca and Hart, 2001) and the mechanisms by which organisms re-attach to the benthos (Fingerut et al., 2006, 2011). We suspect that the addition of such behavioral complexities would manifest themselves in field conditions as increased longitudinal variance in dispersal distances, much like what simple turbulence induces. Indeed, the dispersion we include in our particle tracking simulation allows it to generate a wide distribution of dispersal distances that qualitatively matches those observed in the literature, which are typically fit well by an exponential distribution (McLay, 1970; Elliott, 1971a; Ciborowski 1983; Larkin and McKone 1985; Allan and Feifarek, 1989; Lancaster et al., 1996).

We assumed that our drifting particles were released at 40% of the cell height, which in turn varied across the river cross-section. We recommend careful examination of the effects of introduction and drift height on distances traveled in empirical application, as this parameter could strongly influence dispersal distances (McNair et al., 1997). Given the simplicity of the Merced River, the expected result of releasing particles at, say, the water surface would be a slight increase in the travel distance due to the higher velocity at the surface, but little difference in the qualitative pattern of settlement. A more diffuse vertical distribution of drifting invertebrates would likely lead to higher longitudinal dispersion. However, the assumptions behind this expectation remain to be tested on invertebrates in the field, which is a high priority for our future work.

Stream invertebrates may be highly mobile on the benthos in addition to drifting, exhibiting undirected or upstream-biased crawling (Elliott, 1971b, 2003; Englund and Hamback, 2004; Williams and Williams, 1993). Modelling benthic movement can be accomplished by introducing a diffusion term to the lower equation of Eq. (7). Like with diffusion in the drift, benthic crawling should homogenize small-scale variation in invertebrate densities unless movements respond strongly to local environmental gradients (e.g. patchy food sources). Benthic invertebrates may also initiate emigration at higher rates in response to unfavorable local environmental conditions. Increased emigration may occur in areas of adverse hydrology (Fonseca and Hart, 1996; Wilcox et al., 2008; Winterbottom et al., 1997) or high predation pressure (Englund, 2005; Englund et al., 2001) that occurs in lower velocity areas (Hill and Grossman, 1993; Hughes, 1992; Malmqvist and Sackmann, 1996). The latter is especially important in the context of our simple prediction that macroinvertebrate density should be inversely proportional to flow velocity. Strong emigration responses in low flow areas could weaken or even invert the predictions we make regarding flow and density. Furthermore, drift propensity and habitat associations may differ among larval stages (Elliott, 2008a,b; Lancaster et al., 2011), which could obscure drivers behind patterns in the drift if they are assumed to be age-independent.

The potentially complex movement ecology of macroinvertebrates underscores the need for careful parameterization and validation of models used in flow management contexts. A long-standing criticism of traditional habitat-based EFA methods is that they have been not been adequately tested (Anderson et al., 2006b; Locke et al., 2008). Developing theory based on ecological dynamics has great potential for EFAs, yet – like traditional methods – it requires empirical scrutiny as a component of implementation. For example, particle tracking models have long-standing application in geomorphology and hydrological engineering, yet the simple fact that aquatic macroinvertebrates can alter their behavior in the drift complicates application of particle tracking to ecological contexts. We have shown how key parameters (settling velocities and settling rates) can be extracted from studies of invertebrate drift behavior and have predictable consequences for reach scale distributions. When applied to a specific system, such studies could be informative when applied to the dominate prey taxa for focal fish species (e.g. Baetid mayflies for salmon in the Merced). This could include laboratory studies of settling velocities and drift behavior (e.g. Fonseca 1999; Hayes et al., 2007; Oldmeadow et al., 2010) or experimental drift releases in the field (e.g. studies in Fig. 3). Field validations of drift models should include standard sampling of drift and benthic densities. As an example, Hayes et al. (2007) included laboratory studies of settling velocities and field validations of drift densities to parameterize a pool-level model of drift delivery in a New Zealand river. Because of the central focus on flow needs, drift experiments and field validation should be conducted over a range of flow conditions, as is standard in hydrogeomorphology (see Section 3.2.2). Processing macroinvertebrate survey samples is notoriously time-intensive, yet very large expense and effort are directed towards physical habitat assessments in EFAs; shifting some of these resources towards quantifying basic ecological rates could provide disproportionate benefits.

Included in our exploration of the reach-scale population response to flow variability are transfer functions and a component length scale, the response length. Transfer functions, such as Eq. (13), illustrate how spatial variation can interact with dispersal to alter ecological dynamics across spatial scales. Analyses

of transfer functions provide insights into what spatial scales of environmental variation are likely to dominate a population or community response. The output of Eq. (13) is similar to dynamics observed in previous theory, where environmental variability influencing movement rates (e.g. emigration, settlement) has the strongest population response over small spatial scales and is weak or absent over much larger scales (Anderson et al., 2005, 2008; Nisbet et al., 2007; Diehl et al., 2008). In contrast, variability influencing demographic rates such as births and mortality causes a stronger response over the largest spatial scales and a weaker response over smaller ones. Transfer functions for all of these relationships are straightforward to calculate, and can simultaneously describe the responses to multiple environmental drivers (Nisbet et al., 2007). For example, it should be possible to predict contrasting responses of flow variability on settlement, emigration, and mortality by predation in different flow regimes. We view incorporation of these factors into the modelling framework we have described as a fitting and exciting next step.

Response lengths emerge as a characteristic length scale because of the role they play in defining what are "small" and "large" scale ecological responses. Specifically, they set the spatial scale over which population responses – as defined by the transfer function – transition between those driven by small scale (movement) processes and those by large scale (birth/death) ones. In our results, the dominant scale of flow variability was generally less than the presented response lengths. This fact limited the scale dependencies among models with different parameters as well as among discharge levels, making qualitative relationships between flow and drift availability quite straightforward. This could potentially be a general result, as the rough magnitudes of the response lengths we consider are generally consistent with other published estimates. Response lengths are approximately the average lifetime dispersal distance of organisms that disperse often in the absence of strong density-dependence (Anderson et al., 2006a, 2005; Nisbet et al., 2007); literature values of such distances are ~1–2 km (Hershey et al., 1993; Humphries and Ruxton, 2003), although rougher estimates for several taxa in a high-altitude stream suggest smaller response lengths ~1–200 m (Diehl et al., 2008). It is likely only for species with very high local retention and hence the smallest of response lengths where little effect of flow variability on drift availability would be evident. In these cases, recruitment and mortality influences would be highly prominent at the local scale. Understanding the scale over which these different ecological factors are most likely to manifest can help determine the appropriate scale for sampling in the context of environmental flow assessments or river restoration efforts.

Acknowledgments

The authors wish to thank John Williams, Tom Dunne, Lindsey Albertson, Brad Cardinale, and Laure Pecquerie for very helpful discussions, and Lindsey Albertson for access to data that assisted us in model parameterization. We also thank Jonathan Sarhad, Margaret Simon, and Cincin Young for technical assistance and manuscript preparation. Steven Lindley, Jill Lancaster, Andrew Paul, and three anonymous reviewers provided extremely helpful comments on a previous report on which this manuscript in based, and David Boughton and Mark Henderson provided constructive feedback on an earlier draft of this manuscript. This research was supported and funded by the Public Interest Energy Research Program of the California Energy Commission through the Instream Flow Assessment Program of the Center of Aquatic Biology and Aquaculture of the University of California, Davis, contract number 500-02-004 to RMN and KEA.

References

Abbe, T.B., Montgomery, D.R., 1996. Large woody debris jams, channel hydraulics and habitat formation in large rivers. Regul River 12, 201–221.
Albertson, L.K., Cardinale, B.J., Zeug, S.C., Harrison, L.R., Lenihan, H.S., Wydzga, M.A., 2011. Impacts of channel reconstruction on invertebrate assemblages in a restored river. Restor. Ecol. 19, 627–638.
Allan, J.D., Feifarek, B.P., 1989. Distances traveled by drifting mayfly nymphs—factors influencing return to the substrate. J. N. Am. Benthol. Soc. 8, 322–330.
Anderson, K.E., Hilker, F.M., Nisbet, R.M., 2012. Directional biases and resource-dependence in dispersal generate spatial patterning in a consumer-producer model. Ecol. Lett. 15, 209–217.
Anderson, K.E., Nisbet, R.M., Diehl, S., 2006a. Spatial scaling of consumer–resource interactions in advection-dominated systems. Am. Nat. 168, 358–372.
Anderson, K.E., Nisbet, R.M., Diehl, S., Cooper, S.D., 2005. Scaling population responses to spatial environmental variability in advection-dominated systems. Ecol. Lett. 8, 933–943.
Anderson, K.E., Nisbet, R.M., McCauley, E., 2008. Transient responses to spatial perturbations in advective systems. Bull. Math. Biol. 70, 1480–1502.
Anderson, K.E., Paul, A.J., McCauley, E., Jackson, L.J., Post, J.R., Nisbet, R.M., 2006b. Instream flow needs in streams and rivers: the importance of understanding ecological dynamics. Front. Ecol. Environ. 4, 309–318.
Armstrong, J.D., Nislow, K.H., 2012. Modelling approaches for relating effects of change in river flow to populations of Atlantic salmon and brown trout. Fish. Manage. Ecol. 19, 527–536.
Arthington, A.H., Bunn, S.E., Poff, N.L., Naiman, R.J., 2006. The challenge of providing environmental flow rules to sustain river ecosystems. Ecol. Appl. 16, 1311–1318.
Ayllon, D., Almodovar, A., Nicola, G.G., Parra, I., Elvira, B., 2012. Modelling carrying capacity dynamics for the conservation and management of territorial salmonids. Fish. Res. 134, 95–103.
Bernhardt, E.S., Palmer, M.A., Allan, J.D., Alexander, G., Barnas, K., Brooks, S., Carr, J., Clayton, S., Dahm, C., Follstad-Shah, J., Galat, D., Gloss, S., Goodwin, P., Hart, D., Hassett, B., Jenkinson, R., Katz, S., Kondolf, G.M., Lake, P.S., Lave, R., Meyer, J.L., O'Donnell, T.K., Pagano, L., Powell, B., Sudduth, E., 2005. Ecology—synthesizing US river restoration efforts. Science 308, 636–637.
Breckling, B., Middelhoff, U., Reuter, H., 2006. Individual-based models as tools for ecological theory and application: understanding the emergence of organisational properties in ecological systems. Ecol. Modell. 194, 102–113.
C.A.D.W.R., 2005. The Merced River Salmon Habitat Enhancement Project: Robinson Reach Phase III. California Department of Water Resources, San Joaquin District, Fresno, CA. pp. 159.
Campbell, R.N.B., 1985. Comparison of the drift of live and dead baetis nymphs in a weakening water current. Hydrobiologia 126, 229–236.
Chipps, S.R., Wahl, D.H., 2008. Bioenergetics modeling in the 21st century: reviewing new insights and revisiting old constraints. T. Am. Fish. Soc. 137, 298–313.
Ciborowski, J.J.H., 1983. Influence of current velocity, density, and detritus on drift of 2 mayfly species (Ephemeroptera). Can. J. Zool.—Rev. Can. Zool. 61, 119–125.
D.H.I., 2011. MIKE 21 Flow Model FM. Horsholm, Denmark, pp. 56.
D.H.I., 2011. MIKE 21 Flow Model FM: Particle Tracking Module. Horsholm, Denmark, pp. 48.
Dahl, J., 1998a. Effects of a benthivorous and a drift-feeding fish on a benthic stream assemblage. Oecologia 116, 426–432.
Dahl, J., 1998b. The impact of vertebrate and invertebrate predators on a stream benthic community. Oecologia 117, 217–226.
Dahl, J., Greenberg, L., 1996. Impact on stream benthic prey by benthic vs drift feeding predators: a meta-analysis. Oikos 77, 177–181.
Daufresne, M., Renault, O., 2006. Population fluctuations, regulation and limitation in stream-living brown trout. Oikos 113, 459–468.
Diehl, S., Anderson, K., Nisbet, R.M., 2008. Population responses of drifting stream invertebrates to spatial environmental variability: new theoretical developments. In: Lancaster, J., Briers, R.A. (Eds.), Aquatic Insects: Challenges to Populations. CABI Publishing, Oxfordshire, U.K., pp. 158–183.
Elliott, J.M., 1971a. The distances travelled by drifting invertebrates in a Lake District stream. Oecologia 6, 350–379.
Elliott, J.M., 1971b. Upstream movements of benthic invertebrates in a Lake District stream. J. Anim. Ecol. 40, 235–&.
Elliott, J.M., 2003. A comparative study of the dispersal of 10 species of stream invertebrates. Freshwater Biol. 48, 1652–1668.
Elliott, J.M., 2008a. Ontogenetic changes in the drifting of four species of elmid beetles elucidate the complexity of drift-benthos relationships in a small stream in Northwest England. Freshwater Biol. 53, 159–170.
Elliott, J.M., 2008b. Ontogenetic shifts in drift periodicity and benthic dispersal in elmid beetles. Freshwater Biol. 53, 698–713.
Englund, G., 2005. Scale dependent effects of predatory fish on stream benthos. Oikos 105, 31–40.
Englund, G., Cooper, S.D., Sarnelle, O., 2001. Application of a model of scale dependence to quantify scale domains in open predation experiments. Oikos 92, 501–514.
Englund, G., Hamback, P.A., 2004. Scale-dependence of movement rates in stream invertebrates. Oikos 105, 31.
Fingerut, J.T., Hart, D.D., McNair, J.N., 2006. Silk filaments enhance the settlement of stream insect larvae. Oecologia 150, 202–212.
Fingerut, J.T., Hart, D.D., Thomson, J.R., 2011. Larval settlement in benthic environments: the effects of velocity and bed element geometry. Freshwater Biol. 56, 904–915.

Fonseca, D.M., 1999. Fluid-mediated dispersal in streams: models of settlement from the drift. Oecologia 121, 212–223.
Fonseca, D.M., Hart, D.D., 1996. Density-dependent dispersal of black fly neonates is mediated by flow. Oikos 75, 49–58.
Fonseca, D.M., Hart, D.D., 2001. Colonization history masks habitat preferences in local distributions of stream insects. Ecology 82, 2897–2910.
Frank, B.M., Piccolo, J.J., Baret, P.V., 2011. A review of ecological models for brown trout: towards a new demogenetic model. Ecol. Freshwater Fish. 20, 167–198.
Grossman, G.D., Rincon, P.A., Farr, M.D., Ratajczak, R.E., 2002. A new optimal foraging model predicts habitat use by drift-feeding stream minnows. Ecol. Freshwater Fish. 11, 2–10.
Gurnell, A.M., Piegay, H., Swanson, F.J., Gregory, S.V., 2002. Large wood and fluvial processes. Freshwater Biol. 47, 601–619.
Harrison, L.R., Legleiter, C.J., Wydzga, M.A., Dunne, T., 2011. Channel dynamics and habitat development in a meandering, gravel bed river. Water Resour. Res. 47.
Hart, D.D., Finelli, C.M., 1999. Physical-biological coupling in streams: the pervasive effects of flow on benthic organisms. Annu. Rev. Ecol. Syst. 30, 363–395.
Hayes, J.W., Hughes, N.F., Kelly, L.H., 2007. Process-based modelling of invertebrate drift transport, net energy intake and reach carrying capacity for drift-feeding salmonids. Ecol. Modell. 207, 171–188.
Hershey, A.E., Pastor, J., Peterson, B.J., Kling, G.W., 1993. Stable isotopes resolve the drift paradox for baetis mayflies in an arctic river. Ecology 74, 2315–2325.
Hill, J., Grossman, G.D., 1993. An energetic model of microhabitat use for rainbow-trout and rosyside dace. Ecology 74, 685–698.
Hughes, N.F., 1992. Selection of positions by drift-feeding salmonids in dominance hierarchies—model and test for arctic grayling (*Thymallus arcticus*) in sub-arctic mountain streams, interior alaska. Can. J. Fishe. Aquat. Sci. 49, 1999–2008.
Hughes, N.F., 1998. A model of habitat selection by drift-feeding stream salmonids at different scales. Ecology 79, 281–294.
Humphries, S., Ruxton, G.D., 2003. Estimation of intergenerational drift dispersal distances and mortality risk for aquatic macroinvertebrates. Limnol. Oceanogr. 48, 2117–2124.
Kolpas, A., Nisbet, R.M., 2010. Effects of demographic stochasticity on population persistence in advective media. Bull. Math. Biol. 72, 1254–1270.
Kooijman, S.A.L.M., 2010. Dynamic Energy Budget Theory for Metabolic Organisation, 3rd ed. Cambridge University Press, U.K.
Lamouroux, N., Capra, H., Pouilly, M., Souchon, Y., 1999. Fish habitat preferences in large streams of southern France. Freshwater Biol. 42, 673-673.
Lancaster, J., Downes, B.J., Arnold, A., 2011. Lasting effects of maternal behaviour on the distribution of a dispersive stream insect. J. Anim. Ecol. 80, 1061–1069.
Lancaster, J., Hildrew, A.G., Gjerlov, C., 1996. Invertebrate drift and longitudinal transport processes in streams. Can. J. Fish. Aquat. Sci. 53, 572–582.
Larkin, P.A., McKone, D.W., 1985. An evaluation by field experiment of the McLay model of stream drift. Can. J. Fish. Aquat. Sci. 42, 909–918.
Legleiter, C.J., Harrison, L.R., Dunne, T., 2011. Effect of point bar development on the local force balance governing flow in a simple, meandering gravel bed river. J. Geophys. Res.—Earth 116.
Legleiter, C.J., Kyriakidis, P.C., 2008. Spatial prediction of river channel topography by kriging. Earth Surf. Process. Landforms 33, 841–867.
Locke, A., Stalnaker, C., Zellmer, S., Williams, K., Beecher, H., Richards, T., Robertson, C., Wald, A., Paul, A., Annear, T., 2008. Integrated Approaches to Riverine Resource Management: Case Studies, Science, Law, People, and Policy. Instream Flow Council, Cheyenne, WY.
Lutscher, F., Pachepsky, E., Lewis, M.A., 2005. The effect of dispersal patterns on stream populations. SIAM Rev. 47, 749–772.
Lytle, D.A., Poff, N.L., 2004. Adaptation to natural flow regimes. Trends Ecol. Evol. 19, 94–100.
Malmqvist, B., Sackmann, G., 1996. Changing risk of predation for a filter-feeding insect along a current velocity gradient. Oecologia 108, 450–458.
McLay, C., 1970. A theory concerning the distance traveled by animals entering the drift of a stream. J. Fish. Res. Board Can. 27, 359–370.
McNair, J.N., Newbold, J.D., Hart, D.D., 1997. Turbulent transport of suspended particles and dispersing benthic organisms: how long to hit bottom? J. Theor. Biol. 188, 29–52.
Milhous, R.T., Waddle, T.J., 2012. Physical Habitat Simulation (PHABSIM) Software for Windows (v.1.5.1). USGS Fort Collins Science Center, Fort Collins, CO.
Nelson, J.M., McDonald, R.R., 1996. Mechanics and modeling of flow and bed evolution in lateral separation eddies. In: G.C.M.a.R.C. (Ed.), United States Geological Survey. Flagstaff, AZ, pp. 69.
Nelson, J.M., Bennett, J.P., Wiele, S.M., 2003. Flow and sediment transport modeling. In: Kondolf, G.M., Piegay, H. (Eds.), Tools in Fluvial Geomorphology. Wiley, Chichester, pp. 539–576.
Ney, J.J., 1993. Bioenergetics modeling today—growing pains on the cutting edge. T Am. Fish. Soc. 122, 736–748.
Nisbet, R.M., Anderson, K.E., McCauley, E., Lewis, M.A., 2007. Response of equilibrium states to spatial environmental heterogeneity in advective systems. Math. Biosci. Eng. 4, 1–13.
Nisbet, R.M., Jusup, M., Klanjscek, T., Pecquerie, L., 2012. Integrating dynamic energy budget (DEB) theory with traditional bioenergetic models. J. Exp. Biol. 215, 892–902.
Oldmeadow, D.F., Lancaster, J., Rice, S.P., 2010. Drift and settlement of stream insects in a complex hydraulic environment. Freshwater Biol. 55, 1020–1035.
Otto, C., Sjostrom, P., 1986. Behavior of drifting insect larvae. Hydrobiologia 131, 77–86.
Pachepsky, E., Lutscher, F., Nisbet, R.M., Lewis, M.A., 2005. Persistence, spread and the drift paradox. Theor. Population Biol. 67, 61.
Pecquerie, L., Johnson, L.R., Kooijman, S., Nisbet, R.M., 2011. Analyzing variations in life-history traits of Pacific salmon in the context of Dynamic Energy Budget (DEB) theory. J. Sea Res. 66, 424–433.
Poff, N.L., Allan, J.D., Bain, M.B., Karr, J.R., Prestegaard, K.L., Richter, B.D., Sparks, R.E., Stromberg, J.C., 1997. The natural flow regime. BioScience 47, 769–784.
Poff, N.L., Richter, B.D., Arthington, A.H., Bunn, S.E., Naiman, R.J., Kendy, E., Acreman, M., Apse, C., Bledsoe, B.P., Freeman, M.C., Henriksen, J., Jacobson, R.B., Kennen, J.G., Merritt, D.M., O'Keeffe, J.H., Olden, J.D., Rogers, K., Tharme, R.E., Warner, A., 2010. The ecological limits of hydrologic alteration (ELOHA): a new framework for developing regional environmental flow standards. Freshwater Biol. 55, 147–170.
Richter, B.D., Warner, A.T., Meyer, J.L., Lutz, K., 2006. A collaborative and adaptive process for developing environmental flow recommendations. River Res. Appl. 22, 297–318.
Rodi, W., 1993. Turbulence Models and Their Application in Hydraulics: A State-of-the-Art Review, third ed. A.A. Balkema, Rotterdam.
Rosenfeld, J.S., Taylor, J., 2009. Prey abundance, channel structure and the allometry of growth rate potential for juvenile trout. Fish. Manage. Ecol. 16, 202–218.
Shenton, W., Bond, N.R., Yen, J.D.L., Mac Nally, R., 2012. Putting the "ecology" into environmental flows: ecological dynamics and demographic modelling. Environ. Manage. 50, 1–10.
Speirs, D.C., Gurney, W.S.C., 2001. Population persistence in rivers and estuaries. Ecology 82, 1219–1237.
Tharme, R.E., 2003. A global perspective on environmental flow assessment: emerging trends in the development and application of environmental flow methodologies for rivers. River Res. Appl. 19, 397–441.
Townsend, C.R., 1989. The patch dynamics concept of stream community ecology. J. N. Am. Benthol. Soc. 8, 36–50.
Van Winkle, W., Jager, H.I., Railsback, S.F., Holcomb, B.D., Studley, T.K., Baldrige, J.E., 1998. Individual-based model of sympatric populations of brown and rainbow trout for instream flow assessment: model description and calibration. Ecol. Modell. 110, 175–207.
Vannote, R.L., Minshall, G.W., Cummins, K.W., Sedell, J.R., Cushing, C.E., 1980. The river continuum concept. Can. J. Fish. Aquat. Sci. 37, 130–137.
Vincenzi, S., Crivelli, A.J., Jesensek, D., De Leo, G.A., 2008. The role of density-dependent individual growth in the persistence of freshwater salmonid populations. Oecologia 156, 523–534.
Wilcox, A.C., Peckarsky, B.L., Taylor, B.W., Encalada, A.C., 2008. Hydraulic and geomorphic effects on mayfly drift in high-gradient streams at moderate discharges. Ecohydrology 1, 176–186.
Williams, D.D., Williams, N.E., 1993. The upstream/downstream movement paradox of lotic invertebrates: quantitative evidence from a Welsh mountain stream. Freshwater Biol. 30, 199–218.
Winterbottom, J., Orton, S., Hildrew, A., 1997. Field experiments on the mobility of benthic invertebrates in a southern English stream. Freshwater Biol. 38, 37–47.
Woodward, G.U.Y., Hildrew, A.G., 2002. Food web structure in riverine landscapes. Freshwater Biol. 47, 777–798.
Wu, W., 2008. Computational River Dynamics. Taylor & Francis, London, UK.